DESIGN AND ANALYSIS
OF A
LOW FREQUENCY FM DEMODULATOR

by

Richard Calvin Dean

A Thesis Submitted to the Faculty of the

DEPARTMENT OF ELECTRICAL ENGINEERING

In Partial Fulfillment of the Requirements
For the Degree of

MASTER OF SCIENCE

In the Graduate College

THE UNIVERSITY OF ARIZONA

1 9 6 7

STATEMENT BY AUTHOR

This thesis has been submitted in partial fulfillment of requirements for an advanced degree at The University of Arizona and is deposited in the University Library to be made available to borrowers under rules of the Library.

Brief quotations from this thesis are allowable without special permission, provided that accurate acknowledgment of source is made. Requests for permission for extended quotation from or reproduction of this manuscript in whole or in part may be granted by the head of the major department or the Dean of the Graduate College when in his judgment the proposed use of the material is in the interests of scholarship. In all other instances, however, permission must be obtained from the author.

SIGNED: Richard C Dean

APPROVAL BY THESIS DIRECTOR

This thesis has been approved on the date shown below:

W. H. Evans

W. H. EVANS
Professor of Electrical Engineering

May 11, 1967
Date

ACKNOWLEDGEMENT

The author is grateful to Professor Walter H. Evans whose guidance, assistance, and encouragement made this project possible.

TABLE OF CONTENTS

LIST OF ILLUSTRATIONS

LIST OF TABLES

ABSTRACT

This thesis presents a method of demodulating a frequency modulated signal having a bandwidth and center frequency of 400 hertz. Essentially, the demodulator input is a sine wave obtained from the playback head of a tape recorder, and the output is a DC voltage level which varies up to 60 hertz.

The input signal is amplified and clipped to form a square wave which is differentiated and used to trigger a monostable multivibrator. The multivibrator is basically a bistable circuit having an attached delayed pulse generator for the purpose of triggering the multivibrator to the quiescent state at the end of a specified period. This arrangement provides superior frequency stability. The multivibrator output is fed into an active low-pass filter to remove the carrier wave and then to a voltage display to gain the desired information.

CHAPTER 1

INTRODUCTION

1.1 The Problem and Justification

Information contained in a frequency modulated signal having a bandwidth and center frequency of 400 hertz must be recovered. This thesis presents the design and analysis of a demodulator capable of accomplishing this task.

Studies in the field of atmospheric electricity require large quantities of information to be stored for analysis and interpretation at a later time. This demodulator is to be used as the playback circuitry of a seven channel low speed (½ inch per second) tape recorder for use in these studies.

The input to the tape system is an analog signal varying in level between ±1 volt at a rate of 0 to 60 hertz. This signal is converted by the recording circuitry so that the tape head input is a frequency modulated signal consisting of 22.5 microsecond pulses varying in frequency from 200 to 600 hertz at a rate of 0 to 60 hertz.

Much fidelity is lost in both recording and playback due to the slow tape speed. The output from the playback head consists of a distorted sine wave with a 0.4

millivolt peak to peak amplitude having frequency characteristics identical to the tape head input.

1.2 The Demodulator

Demodulation is used to recover the input analog signal from the tape head output. A block diagram of the demodulator is shown in Figure 1.1. The tape head output is amplified (Appendix A) as the first step in demodulation. This signal is then used as the input to a second amplifier which serves the purpose of a clipping circuit (Appendix B) since it is heavily saturated for both the positive and negative portions of the sine wave. The output of this circuit is, therefore, a close approximation of a square wave having a frequency identical to that of the tape head output.

The square wave is differentiated to produce positive and negative pulses. The positive pulse is utilized as a trigger to the input of a monostable multivibrator. The multivibrator output is a pulse which is constant in length and voltage between the two frequency extremes of the FM input signal. The output, therefore, possesses a DC level proportional to the triggering frequency.

The output of the multivibrator is filtered and amplified by the last stage of the demodulator, a low pass active filter. The filter recovers the DC component of the Fourier series representation of the input to the filter.

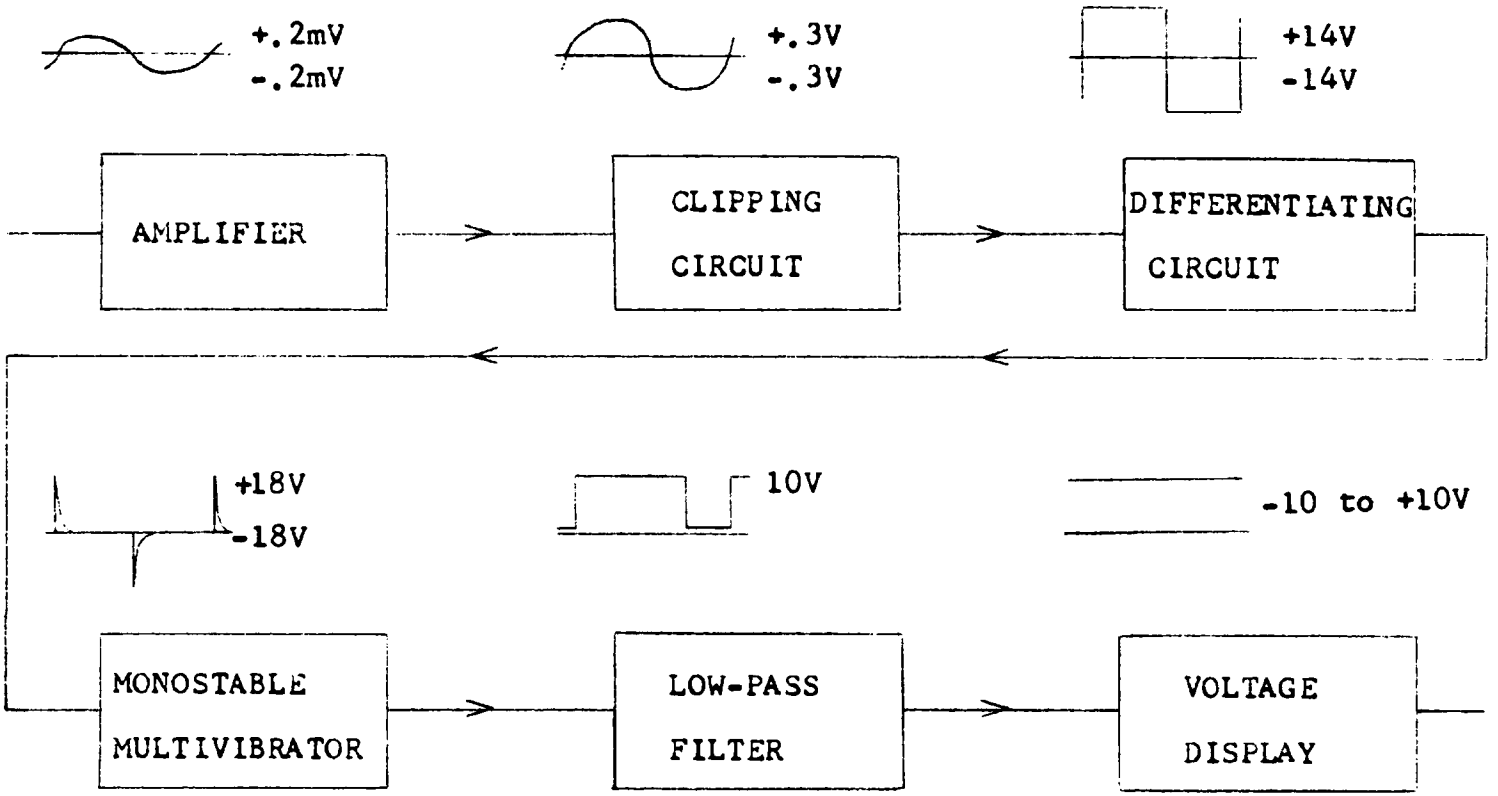

Figure 1.1 Demodulator Block Diagram

The filter output is an analog signal varying between $\pm V$ volts with zero volts corresponding to zero volts into the recording circuitry (Table 1.1).

The output signal of the demodulator is fed to a voltage display circuit where the tape system input signal may be analyzed. The transfer function for the tape system is given by

$$V_{out} = kV_{in}$$

for signal frequencies less than the filter cutoff frequency.

Table 1.1 Input Frequency Versus DC Output Level (Signal Source: Tape Recorder)

Demodulator Input Frequency	Demodulator Output Voltage Level
200 hertz	10.0 ±0.1 volts
300 hertz	5.0 ±0.1 volts
400 hertz	0.0 ±0.2 volts
500 hertz	-5.1 ±0.3 volts
600 hertz	-10.2 ±0.3 volts

CHAPTER 2

A MONOSTABLE MULTIVIBRATOR

2.1 Advantages of a Transistor-Unijunction Multivibrator

The monostable multivibrator is the most critical portion of the circuit. The DC level of the multivibrator output is directly dependent upon both the pulse height and the pulse length. For this reason, care must be taken in the design to insure that both the voltage level and the pulse length are constant under all operating conditions.

In a conventional multivibrator, (Fig. 2.1) the timing capacitor, C_T, must become fully charged in the metastable state if a constant pulse length is to be obtained. Requirements of this demodulator demand that as much of the period be used as possible in order to obtain clearly defined ouput levels. For the frequencies used here, at the minimum 1.67 millisecond period and 1.25 millisecond pulse length, a charge time of only 420 microseconds is allowed. This allows a time constant of less than 100 microseconds for full charge recovery. $R_{c1}C_T$ will normally exceed 100 microseconds in this type circuit; therefore, a circuit independent of frequency must be utilized.

The UJT-transistor multivibrator (Sylvan 1965, pp 54-5) shown in Figure 2.2 overcomes the major disadvantage of

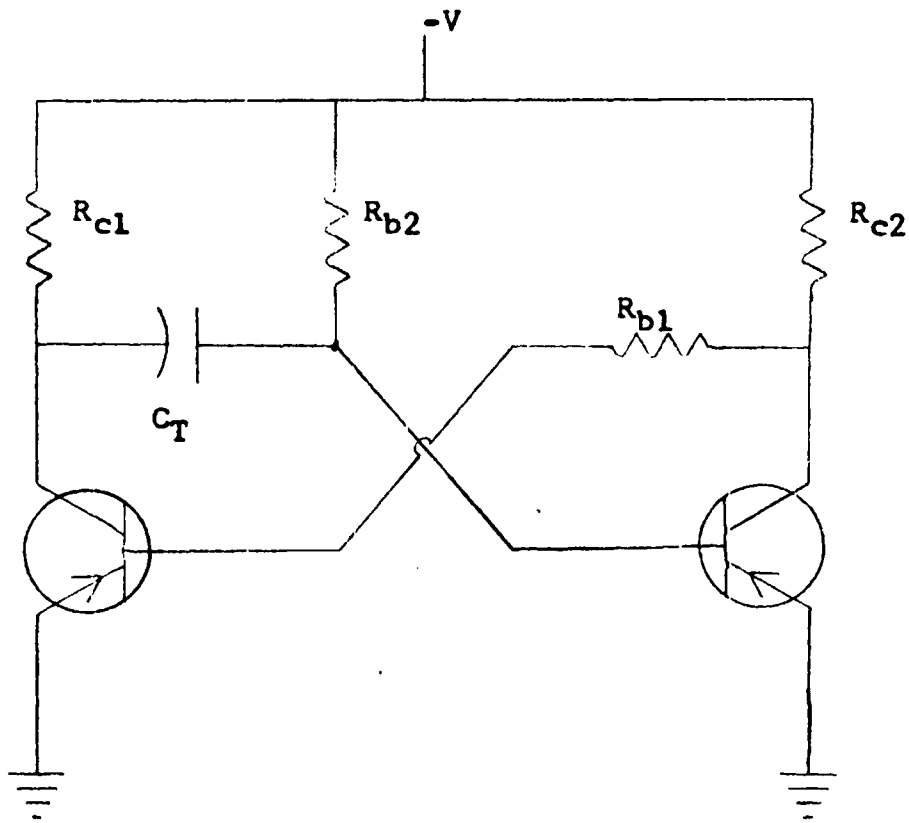

Pulse length = $.69R_{b2}C_T$

Recovery time = $5R_{c1}C_T$

Figure 2.1 Conventional Monostable Multivibrator

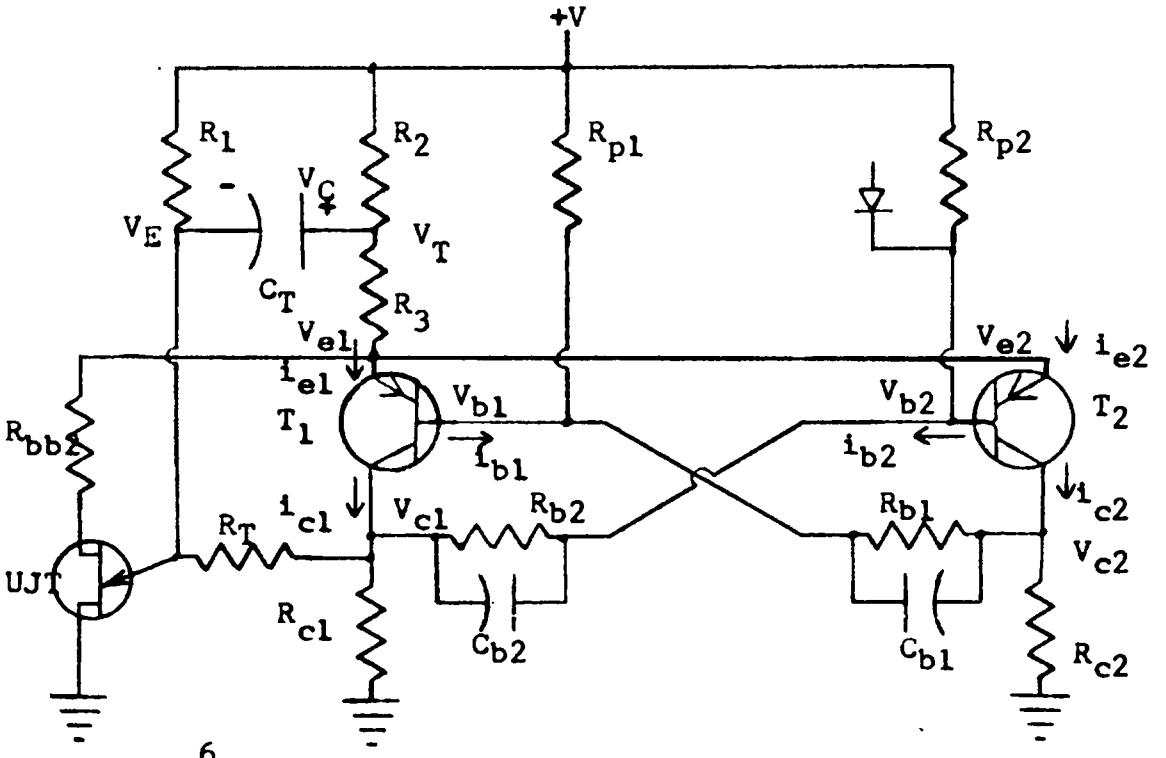

R_1 = 1.2×10^6 ohms
R_2 = 5.6 ohms
R_3 = 275 ohms
$R_{p1} = R_{p2}$ = 47×10^3 ohms
$R_{b1} = R_{b2}$ = 15×10^3 ohms
R_{c2} = 10^3 ohms
R_{c1} = 910 ohms
R_{bb2} = 220 ohms
R_T = 10^5 ohms
R_{bb} = 5.76×10^3 ohms

C_T = .018 microfarads
C_{b1} = .01 microfarads
C_{b2} = .002 microfarads
V = 15 volts
$T_1 = T_2$ = 2N3638A
UJT = 2N489A

All component values are $\pm$10%.

Figure 2.2 UJT-Transistor Monostable Multivibrator

the conventional multivibrator. It retains a stable pulse length regardless of the trigger frequency. The circuit can be most easily envisioned by considering it as a bistable multivibrator which, after being initially triggered, is triggered again after a specified time by a delayed pulse generator.

When the ciruuit of Figure 2.2 is in the quiescent state, T_1 is cutoff and T_2 is saturated. If a positive pulse is applied to the base of T_2, T_2 is turned off. T_1 then becomes saturated, and the circuit enters the active state. V_E in the quiescent state is approximately 2 volts; however, in the active state V_E rises exponentially towards 12 volts with a time constant of R_TC_T. When V_E reaches the firing point, V_p, of the UJT, C_T is rapidly discharged through the UJT and R_2 until the UJT turns off at approximately 2 volts. This produces a negative pulse on the emitters of T_1 and T_2. The pulse turns T_1 off and T_2 is again saturated by the regenerative feedback of the circuit. The circuit is now in the quiescent state and awaits another trigger. A false trigger applied while the circuit is in the active state will have no effect since T_2 is already off.

2.2 Analysis in the Quiescent State

Analysis of the circuit is quite conventional after certain simplifications are made. The calculated numerical values were obtained using exact resistance and capacitance

values obtained from a bridge rather than the nominal values. Utilizing zero order models for the UJT, saturated T_2, and cutoff T_1,

$$V_{e1} = V_{e2} = V_{b2} = V_{c2} \approx V\frac{x}{x+y} = 11.42V$$

where

$$x = R_{c2} \| (R_{b2}+R_{c1}) \| (R_{bb}+R_{bb2})$$

$$y = R_{p2} \| (R_{b1}+R_{p1}) \| (R_2+R_3).$$

From this value, V_{c1} and V_{b1} are found to be

$$V_{c1} = V\frac{R_{c1}}{R_T+R_1+R_{c1}} + V_{b2}\frac{R_{c1}}{R_{c1}+R_{b2}} = .66V$$

$$V_{b1} = V_{c2} + (V-V_{c2})\frac{R_{b1}}{R_{b1}+R_{p1}} = 12.34V.$$

With the above values, i_{b2} and i_{c2} as defined in Figure 2.2 are found as

$$i_{b2} = \frac{V_{b2}-V_{c1}}{R_{b2}} - \frac{V-V_{b2}}{R_{p2}} = .57ma$$

$$i_{c2} = \frac{V_{c2}}{R_{c2}} - \frac{V_{b1}-V_{c2}}{R_{b1}} = 11.42ma.$$

These values result in

$$i_{e2} = i_{b2} + i_{c2} = 11.99ma.$$

Employing a transistor curve tracer and using the appropriate currents for the transistor, the saturation voltages and base current amplification factors for T_2 were determined to be

$$V_{eb} = .69V \qquad \beta_N = 180$$

$$V_{ec} = .051V \qquad \beta_I = 11$$

resulting in

$$\alpha_N = .995 \qquad \alpha_I = .961.$$

A typical I_{CS} for T_1 was obtained from specification sheets as 0.1 nanoamperes. For worst case design analysis, a value an order of magnitude larger, 1 nanoampere, was used. Utilizing the transistor curve tracer for T_1, it was determined that

$$\beta_N = 150 \qquad \beta_I = 5$$

resulting in

$$\alpha_N = .994 \qquad \alpha_I = .834.$$

I_{ES} and I_{CS} are coupled through the reciprocity relationship (Angelo 1964, p. 50)

$$\alpha_N I_{ES} = \alpha_I I_{CS}$$

therefore,

$$I_{ES} = I_{CS} \frac{\alpha_I}{\alpha_N} = .839na.$$

For the next iteration in the circuit analysis, the Ebers-Moll cutoff model (Angelo 1964, p. 41) for T_1 (Fig. 2.3), and the transistor symbol showing the voltage drops (Fig. 2.4) for the saturated T_2 were used.

Specification sheets list typical I_{B2E0} for the UJT as 8 nanoamperes at 30 volts and 50°C. There are approximately 11 volts across R_{bb} in this circuit; therefore, I_{B2E0} is considerably less and may be neglected. The model for the unijunction transistor then may be shown as in Figure 2.5. R_{bb} was measured at 11 volts since R_{bb} varies with V_{bb}.

Utilizing the models of Figures 2.3, 2.4, and 2.5, new current and voltage levels may be obtained. The previously derived value for V_{e2} is assumed to be correct. From these assumptions

$$V_{c2} = V_{e2} - V_{ec} = 11.37V$$

$$V_{b2} = V_{e2} - V_{cb} = 10.78V.$$

The currents of the cutoff transistor (Fig. 2.3) are assumed to be negligible since they are small compared to the approximate currents found in the zero order model. The leakage current of 8 nanoamperes for the UJT is also assumed to be negligible. This results in

$$i_{b2} = \frac{V_{b2}}{R_{b2}+R_{c1}} - \frac{V-V_{b2}}{R_{p2}} = .523ma$$

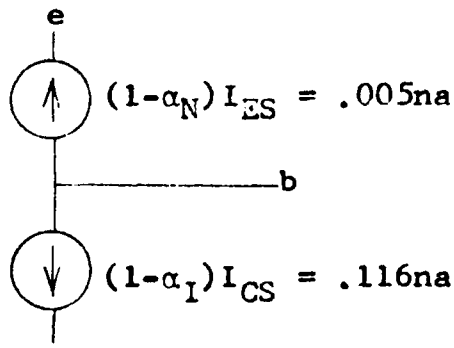

Figure 2.3 Cutoff Transistor

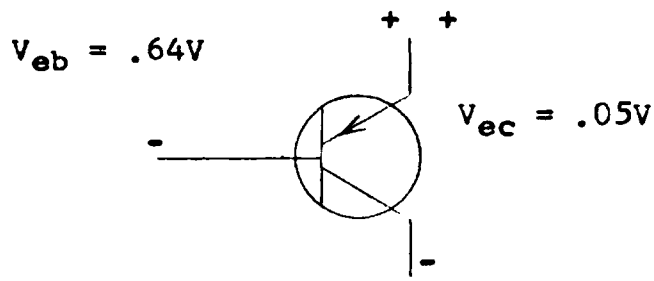

Figure 2.4 Saturated Transistor

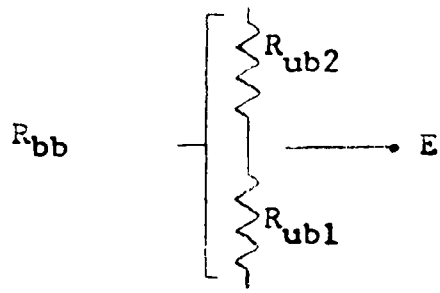

Figure 2.5 Unijunction Transistor Cutoff Model

$$i_{c2} = \frac{V_{c2}}{R_{c2}} - \frac{V-V_{c2}}{R_{b1}+R_{p1}} = 11.34\text{ma}.$$

V_{e2} may now be recalculated.

$$V'_{e2} \approx (R_2+R_3)\left\{ \cancel{i_{e1}}^{0} + i_{b2} + i_{c2} + \frac{V_{e2}}{R_{bb}+R_{bb2}} \right\} = 11.41\text{V}.$$

Utilizing the transistor curve tracer it is determined that

$$V_{ec} = .050\text{V} \qquad V_{eb} = .72\text{V}.$$

This set of values allows a new computation of T_2 voltages

$$V_{c2} = 11.36\text{V} \qquad V_{b2} = 10.69\text{V}.$$

These voltage values, being close to the initially computed values, are assumed to be correct.

Two important values needed from the quiescent state are V_T and V_E as shown in Figure 2.2.

$$V_E = V_{c1} + \frac{R_T}{R_T+R_1}(V-V_{c1}) = 1.71\text{V}$$

where

$$V_{c1} = R_{c1}\frac{V_{b2}}{R_{b2}+R_{c1}} + \frac{V}{R_1+R_T+R_{c1}} = .616\text{V}.$$

V_T may be computed by

$$V_T = V - (V-V_{e2})\frac{R_2}{R_2+R_3} = 15.15\text{V}.$$

It may be noted that T_2 is well into saturation as desired since

$$i_{b2} = .523\text{ma} > \frac{i_c}{\beta} = .0631\text{ma}.$$

2.3 Analysis in the Metastable State

The same procedures were followed in analyzing the circuit of Figure 2.2 in the active state. Utilizing zero order models with T_2 off and T_1 saturated,

$$V_{b1} = V_{e1} = V_{c1} = V_{e2} = V\,\frac{x}{x+y} = 11.39\text{V}$$

where

$$x = (R_{bb}+R_{bb2}) \,||\, R_{c1} \,||\, (R_{b1}+R_{c2})$$

$$y = R_1 \quad (R_2+R_3) \,||\, R_{p1} \,||\, (R_{b2}+R_{p2})$$

and

$$i_{b1} = \frac{V_{b1}}{R_{b1}+R_{c2}} - \frac{V-V_{b1}}{R_{p1}} = .631\text{ma}$$

$$i_{e1} = \frac{V-V_{e1}}{R_2+R_3} - \frac{V_{e1}}{R_{bb}+R_{bb2}} = 12.06\text{ma}$$

$$i_{c1} = i_{e1} - i_{b1} = 11.42\text{ma}.$$

Employing, the transistor curve tracer for T_1 it was determined that

$$V_{ec} = .065\text{V} \qquad V_{eb} = .67\text{V}.$$

If V_{e1} is considered correct, then

$$v_{b1} = V_{e1} - V_{eb} = 10.72V$$

$$V_{c1} = V_{e1} - V_{ec} = 11.33V.$$

The model for the cutoff transistor, T_2, will then have current generators of values

$$(1-\alpha_I) I_{CS} = .084na$$

$$(1-\alpha_N) I_{ES} = .050na.$$

These values may be neglected at the current levels involved.

Using the above data, new current values for T_1 may be computed.

$$i_{b1} = \frac{V_{b1}}{R_{b1}+R_{c2}} - \frac{V-V_{b1}}{R_{p1}} = .575ma$$

$$i_{c1} = \frac{V_{c1}}{R_{c1}} - \frac{V-V_{c1}}{R_{b2}+R_{p2}} - \frac{V}{R_1+R_T} = 11.47ma.$$

Again the reverse emitter current from the UJT has been assumed negligible since it is of the order of 8 nanoamperes.

Using the transistor curve tracer for T_1 it is determined that

$$V_{eb} = .66V \qquad V_{ec} = .068V.$$

A revised V_{e1} may now be calculated.

$$V'_{e1} = (R_2+R_3)\left\{ \overset{\approx 0}{i_{e2}} + i_{e1} + \frac{V_{e1}}{R_{bb}+R_{bb2}} \right\} = 11.40V$$

$$V_{b1} = V_{e1} - V_{eb} = 10.74V$$

$$V_{c1} = V_{e1} - V_{ec} = 11.33V.$$

Again it may be noted T_1 is saturated since

$$i_{b1} = .575ma > \frac{i_{c1}}{\beta} = .0764ma.$$

The desired values are V_T and V_E. If C_T is assumed negligible in this DC analysis, then

$$V_T = V - (i_{e1} + \frac{V_{e1}}{R_{bb}+R_{bb2}}) R_2 = 15.15V$$

$$V_E = V_{c1} + (V-V_{c1}) \frac{R_T}{R_T+R_1} = 11.65V.$$

The firing point voltage, V_p (Fig. 2.6), of the UJT is critical in the determination of pulse length. To find the actual V_p, R_{bb2} was placed in series with R_{ub2} and V_{e1} applied. A voltage was applied to the emitter and raised until the UJT fired. This yielded

$$V_p = 6.6V.$$

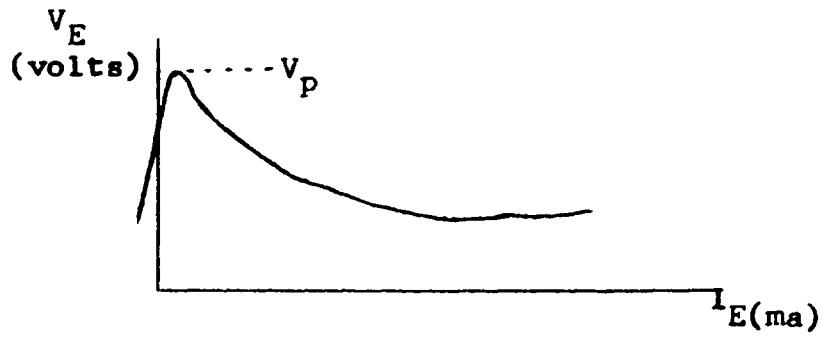

Figure 2.6 Typical Unijunction Emitter Curve

V_T is constant in both the quiescent and active states, and

$$V_T = V_E + V_C.$$

Thus, as V_C exponentially falls when the circuit enters the active state, V_E will rise and

$$V_{E(t)} = V_{Eact} - (V_{Eact} - V_{Equies})e^{\frac{-t}{R_T C_T}}.$$

To find the multivibrator pulse length, $V_{E(t)}$ is replaced by V_p. For $R_T C_T = .0018$ seconds, the pulse length is determined to be

$$t = -R_T C_T \ln \frac{V_p - V_{Eact}}{V_{Equies} - V_{Eact}} = 1.25\text{ms}.$$

At the end of the pulse, the circuit enters the quiescent state where it is stable until triggered again to the active state by a positive pulse on the base of T_2.

2.4 Temperature Dependence

Although the circuit of Figure 2.2 provides a constant pulse length with variations of trigger frequency, it will not do so with variations in temperature.

The pulse length is dependent upon several parameters, one of which, V_p, varies greatly with temperature (Sylvan 1965, pp. 15-24). The UJT peak voltage may be computed by

$$V_p = \gamma V_{bb} + V_D$$

where γ is defined by

$$\gamma = \frac{R_{ub1}}{R_{ub1}+R_{ub2}} = \frac{R_{ub1}}{R_{bb}}.$$

The resistances and voltages are shown in Figure 2.7. R_{ub1} and R_{ub2}, thus R_{bb}, increase almost linearly up to 140°C by the approximate equation.

$$R_{bb}(T_2) = (.008T(^{\circ}C) + .8)\ R_{bb}(T_1)$$

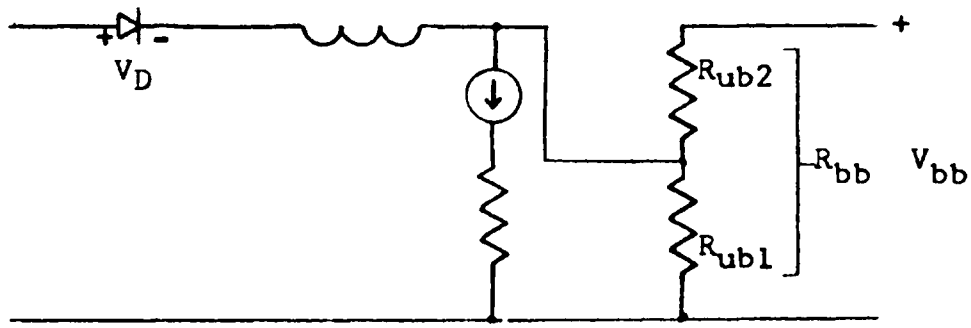

Figure 2.7 A Model for the Unijunction Transistor

This shows γ as being essentially constant with temperature since R_{ub1} and R_{ub2} are made of identical material. V_D is the voltage drop across the diode with I_p flowing in the emitter. V_D is typically 0.7 volts at 25°C and is inversely proportional to temperature with a proportionality constant of approximately 3 millivolts per degree centigrade.

$$V_{D(T)} \approx .7 + .003\ (25-T_2(^{\circ}C)).$$

R_{bb2} stabilizes V_p to some extent since as temperature increases, R_{bb} increases. This causes V_{bb} to increase as V_D falls.

The currents of the cutoff transistor in both the stable and active states will also change with temperature. These currents at the operating temperature of 50°C will increase by a factor of 16 since I_{CS} doubles approximately every 7°C increase in temperature (Angelo 1964, p. 74). They may still be neglected, however, since I_{CS} and I_{ES} are very small at 25°C.

When measured, the circuit experienced a decrease in pulse length of 17 microseconds for a temperature increase from 28°C to 60°C. To minimize this effect the circuit was miniaturized and placed in a temperature controlled (50°C) package.

CHAPTER 3

A LOW-PASS ACTIVE FILTER

A filter is needed to surpress the carrier frequency of the multivibrator output. In addition, amplification is needed to provide easily discernible voltage output levels.

A filter designed by L. Rauch (Foster 1965) meets these needs. The three-pole configuration shown in Figure 3.1 was chosen since it meets the requirements and is an economical active filter design. Additional poles require another operational amplifier for every three poles.

Since the carrier bandwidth extends down to 200 hertz, a requirement of -40 decibels at 200 hertz was imposed. This insures negligible contribution by the carrier to the output level. A pass band of 60 hertz was retained to allow the 0 to 60 hertz input to the recording circuitry to be passed.

Of the three classes of filters, Butterworth, Bessel, and Chebychev, the Chebychev most closely meets the requirements. It has the most rapid cutoff to satisfy the -40 db requirement at 200 hertz and still retain the widest bandwidth.

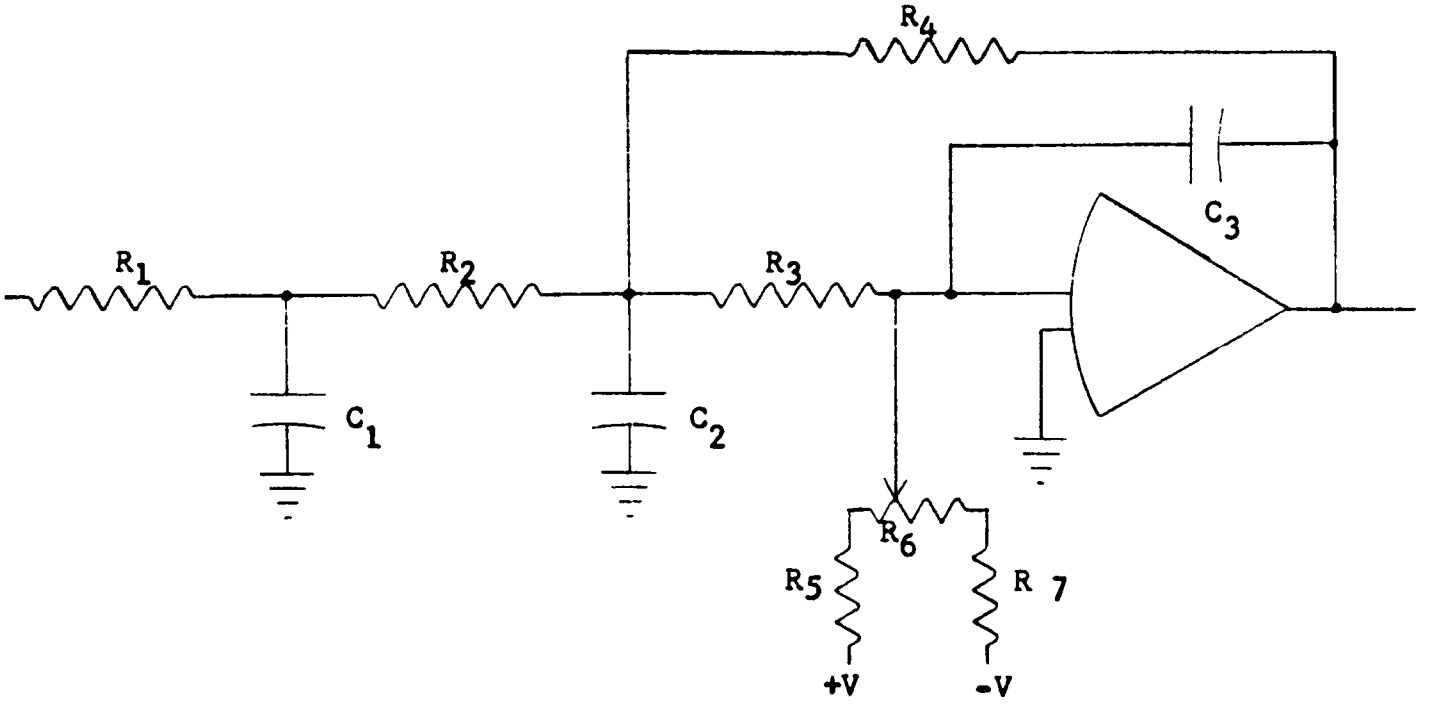

R_1 = $.96 \times 10^5$ ohms
R_2 = $.96 \times 10^5$ ohms
R_3 = 2.9×10^5 ohms
R_4 = 7.2×10^5 ohms
R_5 = 82×10^3 ohms
R_6 = 20×10^3 ohms
R_7 = 82×10^3 ohms

C_1 = .204 microfarads
C_2 = .102 microfarads
C_3 = 335 picafarads
V = 15 volts
Operational Amplifier FU5B770939 651

Figure 3.1 Low-Pass Active Filter

The transfer function of the filter is

$$\frac{E_o}{E_i} = -X^{-1}\left\{ P^3+\left(\frac{R2R_4+R2R3+R3R4}{R_2R_3R_4C_2} + \frac{R_1+R2}{R_1R_2C_1}\right)P^2 \right.$$

$$+\left(\frac{R3R_4+R_2R_4+R_2R_3+R_1R_4+R_1R_3}{R_1R_2R_3R_4C_1C_2} + \frac{1}{R_3R_4C_2C_3}\right)P$$

$$\left. + \frac{R_1+R_2}{R_1R_2R_3R_4C_1C_2C_3}\right\}^{-1}$$

where

$$X = R_1R_2R_3C_1C_2C_3$$

Inserting numerical values, this gives

$$\frac{E_o}{E_i} = -53{,}100{,}000(P^3 + 251P^2 + 149{,}900P + 14{,}200{,}000)^{-1}$$

which has poles of

$$\omega = -105$$

$$\omega = -73 \pm j359.$$

The filter characteristics are shown in Figure 3.2.

A DC voltage level is introduced at the input of the operational amplifier to produce a zero voltage output with 400 hertz input to the demodulator. This allows a voltage swing between $\pm$ 10 volts.

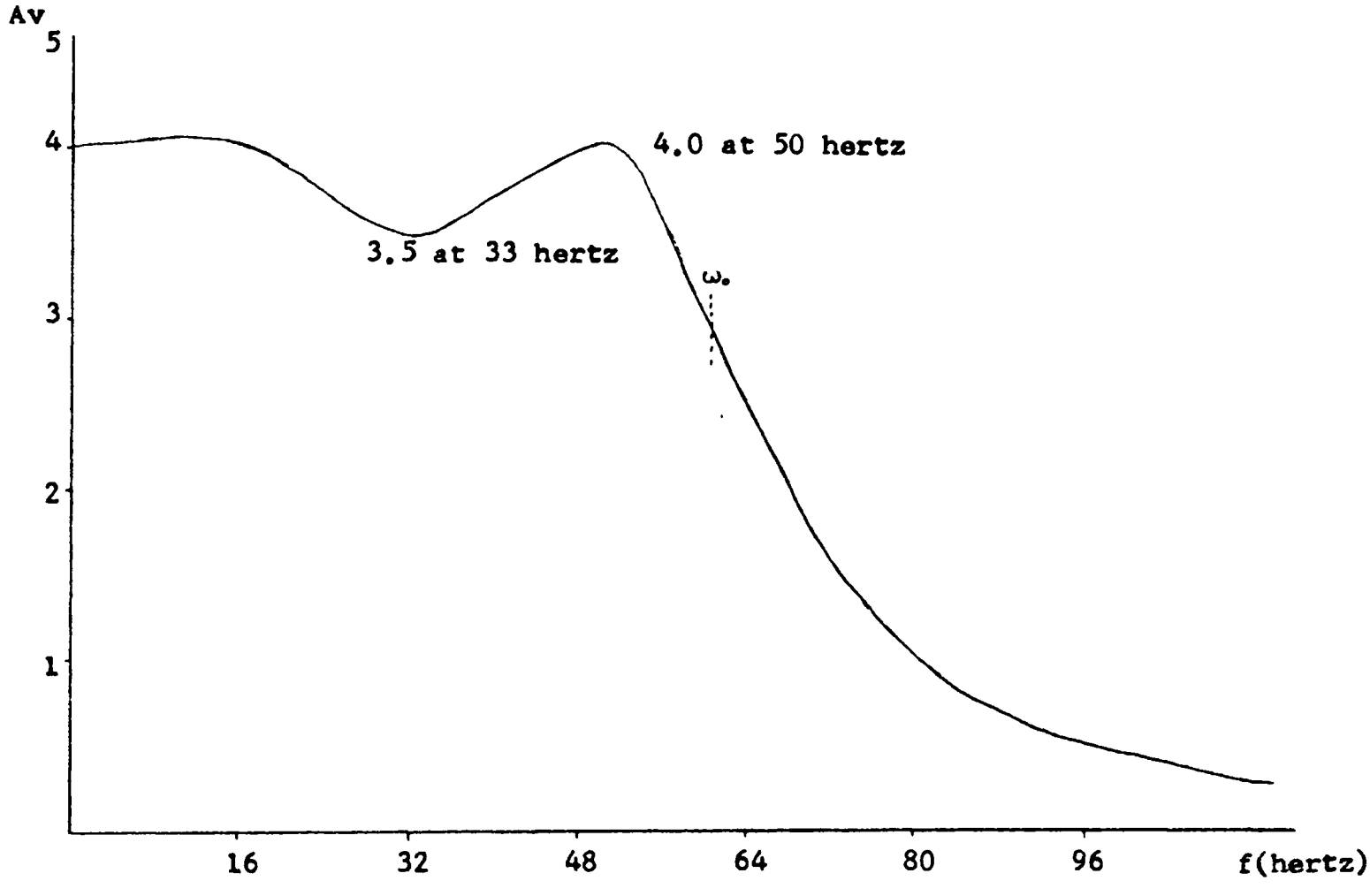

Figure 3.2 Filter Transfer Characteristics

CHAPTER 4

RESULTS, CONCLUSIONS, AND RECOMMENDATIONS

4.1 Results

An FM demodulator capable of recovering an analog signal from the FM tape head output was designed and analyzed in this thesis. Although the demodulator voltage output as listed in Table 1.1 is non-linear, the maximum deviation from linearity is 0.1 volts at the frequency extremes. This results in a system inaccuracy of approximately 1%.

The $\pm$ variations in voltage as shown in Table 1.1 were oscillatory in nature. These oscillations were produced by variations in tape speed during both recording and playback. When a steady frequency source such as an audio oscillator was used as the input to the demodulator, there were no variations in the voltage output level. Table 4.1 shows these results. The system accuracy was improved to better than 0.5%. The major improvement in accuracy was due to the capability of reading the results with less error since the voltage oscillations were absent.

A major cause of the 0.5% inaccuracy was voltage drift of the operational amplifier in the filter circuit. The DC level of the multivibrator, as shown in Table 4.2, was non-linear with an error of only 0.2%. There was no

Table 4.1 Input Frequency Versus DC Output Level
(Signal Source: Audio Oscillator)

Demodulator Input Frequency	Demodulator Output Voltage Level
200 hertz	9.98 volts
300 hertz	4.99 volts
400 hertz	0.00 volts
500 hertz	-4.99 volts
600 hertz	-10.03 volts

Table 4.2 Input Frequency Versus Multivibrator DC Level

Amplifier Input Frequency	Multivibrator DC Level	Adjusted DC Level
200 hertz	3.031 volts	-2.537 volts
300 hertz	4.302 volts	-1.266 volts
400 hertz	5.568 volts	0.000 volts
500 hertz	6.840 volts	1.272 volts
600 hertz	8.114 volts	2.546 volts

drift in this output, therefore, demonstrating the source of drift was the active filter.

The most critical circuit, the UJT-transistor monostable multivibrator, was analyzed in detail. This circuit was demonstrated as being capable of producing an output pulse of 1.25 milliseconds length, with a pulse length deviation of less than 1 microsecond over the frequency band of interest.

4.2 Conclusions and Recommendations

The demodulator is presently capable of detecting a low-frequency FM signal with an error of approximately 1%. If desired, this error may be greatly reduced by incorporating two improvements: one to the tape system and the second to the demodulator.

The tape speed of the recorder should be stabilized to provide an accurate and stable input frequency to the demodulator. Secondly, the accuracy of the demodulator may be greatly increased if the output drift, which is totally attributable to the filter circuit, is reduced. This may be accomplished by replacing the integrated circuit operational amplifier with a more stable operational amplifier such as a chopper stabilized operational amplifier.

Since there will be seven identical channels in the recorder playback system, the demodulator could be made as

a printed circuit. This would facilitate both fabrication and repair of the circuit.

APPENDIX A

AMPLIFICATION

The original 0.4 millivolt peak to peak sine wave input must be amplified to a level where it can be shaped without noise interference. This is done by utilizing an integrated circuit operational amplifier with a feedback resistor (Burr-Brown 1963) as shown in Figure A-1 to give

$$\frac{E_o}{E_{in}} = \frac{R_2}{R_1} = 1500.$$

This gives a peak to peak voltage of 0.6 volts amplitude.

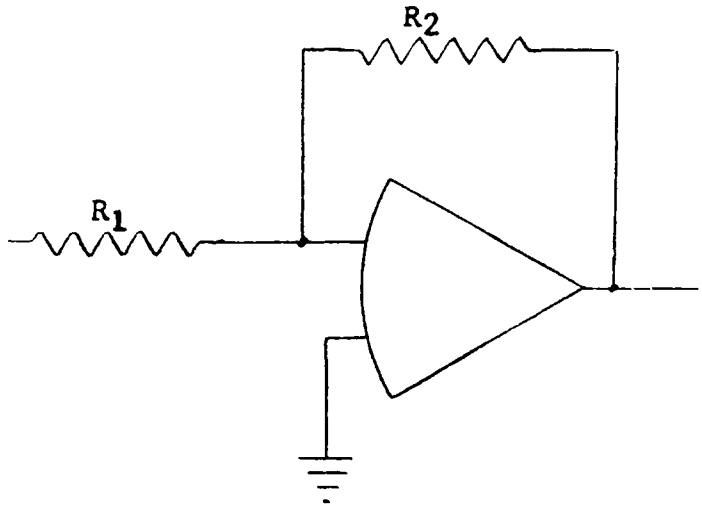

$R_1 = 10^3$ ohms

$R_2 = 1.5 \times 10^6$ ohms

Operational Amplifier-FU5B770939 651

Figure A-1 High Gain Amplifier

APPENDIX B

CLIPPING AND DIFFERENTIATION

The input to the clipping and differentiating stage shown in Figure B-1 is a sine wave of approximately 0.6 volts peak to peak amplitude. The transfer function is

$$\frac{E_o}{E_{in}} = \frac{R_2}{R_1} = 1000.$$

This transfer function gives a theoretical output voltage of 600 volts; however, the operational amplifier is self limiting in voltage (Burr-Brown 1963) and saturates at $\pm$14 volts. This causes the sine wave to be greatly amplified and clipped at $\pm$14 volts to produce a square wave.

The square wave is passed into a differentiating circuit and pulses of 18 volts amplitude and 0.1 milliseconds base width result.

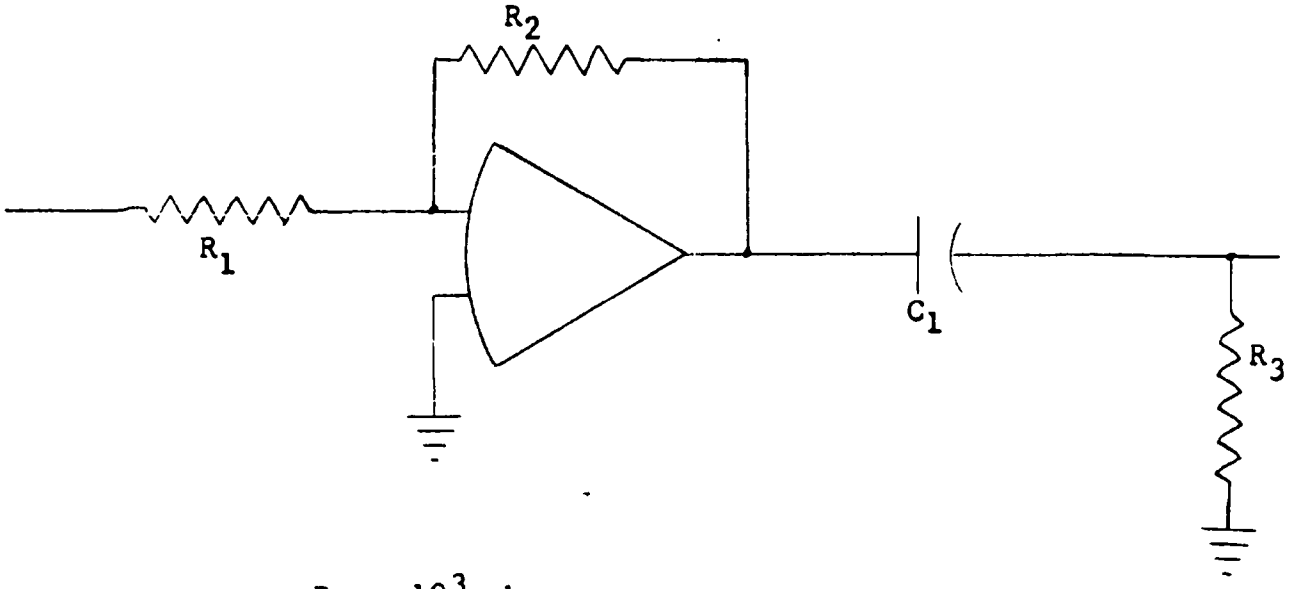

$R_1 = 10^3$ ohms

$R_2 = 10^6$ ohms

$R_3 = 10^4$ ohms

$C_1 = .001$ microfarads

Operational Amplifier-FU5B770939 651

Figure B-1 Amplifier and Clipping Circuit

REFERENCES

1. Angelo, E. J., Jr., A. R. Boothroyd, Paul E. Gray, Donald O. Pederson, and Campbell L. Searle. Elementary Circuit Properties of Transistors, John Wiley and Sons, Inc., 1964.

2. Burr-Brown Applications Engineering Section. Handbook of Operational Amplifier Applications, Burr-Brown Research Corporation, 1963.

3. Foster, Edward J. "Active Low-Pass Filter Design," IEEE Transactions on Audio, AU-13(5) 104-111, 1965.

4. Sylvan, T. P. The Unijunction Transistor Characteristics and Applications, General Electric Company, 1965.